

PACS numbers: 42.55.Px; 41.75.Fr; 42.60.Da; 42.60.Jf; 78.67.De
DOI: 10.1070/QE2012v042n07ABEH014842

Electron beam pumped Zn(Cd)Se/ZnMgSSe quantum well semiconductor disk laser

V.I. Kozlovsky, P.I. Kuznetsov, D.E. Sviridov, G.G. Yakushcheva

Abstract. **We report pulsed 465-nm lasing in a longitudinally electron beam pumped Zn(Cd)Se/ZnMgSSe heterostructure with 30 quantum wells, grown by metalorganic vapour phase epitaxy. At an external spherical mirror radius of 30 mm, 3% transmission of the mirror, and an electron energy of 42 keV, the peak laser output power reached 1.4 W. The pulse duration was 20–40 ns, the emission linewidth was within 0.3 nm, and the beam divergence was about 4–5 mrad, approaching the diffraction limit.**

Keywords: *semiconductor disk laser, electron beam pumping, ZnCdSe/ZnMgSSe heterostructure, quantum well, metalorganic vapour phase epitaxy.*

1. Introduction

The wide use of diode-pumped semiconductor disk lasers is due to their key advantages: good beam directivity, high power, high efficiency, small dimensions and ability to emit light in the visible and UV spectral regions [1–3]. At present, such lasers employ heterostructures that emit in the IR. Visible and near-UV wavelengths can only be obtained through frequency doubling [4, 5], which impairs the laser efficiency and adds complexity to the laser design. The shortest wavelength so far (312.5 nm) has been obtained using a GaInP/AlGaInP heterostructure pumped by a frequency-doubled pulsed neodymium laser [6].

The purpose of this work was to demonstrate a disk laser based on heterostructures of wide band gap II–VI compounds. Unfortunately, laser diodes of sufficient power for pumping structures that emit in the green and blue spectral regions are not yet commercially available. A viable alternative to laser diodes is electron beam pumping. Its efficiency is considerably lower than that of optical pumping, which makes it difficult to achieve cw operation of disk lasers. Because of this, we used pulsed pumping.

V.I. Kozlovsky, D.E. Sviridov P.N. Lebedev Physics Institute, Russian Academy of Sciences, Leninsky prosp. 53, 119991 Moscow, Russia; e-mail: vikoz@sci.lebedev.ru, BonStock@mail.ru;
P.I. Kuznetsov, G.G. Yakushcheva V.A. Kotel'nikov Institute of Radio Engineering and Electronics (Fryazino Branch), Russian Academy of Sciences, pl. Vvedenskogo 1, 141190 Fryazino, Moscow region, Russia; e-mail: pik218@ire216.msk.su, galina@ire216.msk.su

Received 2 March 2012; revision received 10 April 2012
Kvantovaya Elektronika **42** (7) 583–587 (2012)
Translated by O.M. Tsarev

2. Experimental

Figure 1 shows a schematic of the experimental setup. A nanostructure was epoxied to the optical window of the electron beam tube. One mirror was deposited onto the structure and the other was situated on a positioning stage outside the evacuated volume. The electron beam was step-scanned along a short (3 mm) horizontal segment, which in turn could be displaced vertically. In this way, we were able to align the laser by purely electronic means. If the region exposed to the electron beam degraded for some reason, we were able to change the spatial position of the external mirror and, accordingly, the mode position on the gain chip.

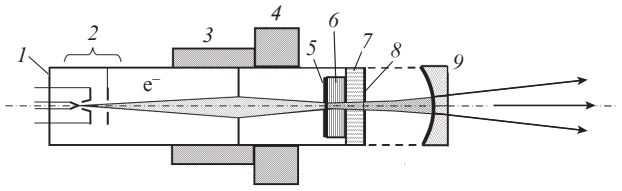

Figure 1. Experimental configuration: (*1*) electron beam tube, (*2*) electron gun, (*3*) deflection coil, (*4*) focusing coil, (*5*) high-reflectivity coating, (*6*) Zn(Cd)Se/ZnMgSSe structure containing 30 quantum wells, (*7*) substrate (output window of the tube), (*8*) anti-reflection coating, (*9*) external mirror.

The nanostructure was grown on a GaAs substrate and included 30 quantum wells (QWs), each about 8 nm in thickness. The QWs were separated by ZnMgSSe barriers 168 nm in nominal thickness. The heterostructure period, $p = 176$ nm, was tuned to the lasing wavelength inside it, λ/N_s, where λ is the wavelength in air and N_s is the average refractive index of the structure. The barrier layers had a low-temperature band gap of about 3.1 eV and were closely lattice-matched to GaAs. The overall thickness of the structure was 5.45 μm. The Cd concentration in the $Zn_{1-x}Cd_xSe$ QWs was $x = 0.04$. The addition of Cd to such QWs improves the cathodoluminescence efficiency of the structure [7]. Moreover, Cd compensates the blue shift of the emission wavelength in ZnSe/ZnMgSSe structures due to Mg diffusion from the barriers to the QWs [8]. The structures were grown by metalorganic vapour phase epitaxy in a laboratory-scale quartz reactor at atmospheric pressure using hydrogen as a carrier gas. Such structures were used earlier to fabricate rather efficient microcavity lasers [7].

In fabricating the gain chip (Fig. 2), the structure was first bonded with Epotek-301 optical epoxy to a sapphire or quartz

substrate, which served as the output window of the electron beam tube. The output surface of the window had anti-reflection coating. Next, the GaAs substrate was removed. A high-reflectivity dielectric mirror composed of 8.5 pairs of quarter-wave SiO_2 and Ta_2O_5 layers and an Al layer 0.1–0.2 μm thick was deposited onto the structure. The QWs were thus located near the antinodes of the generated cavity mode. In this case, the structure ensured resonant periodic gain [9].

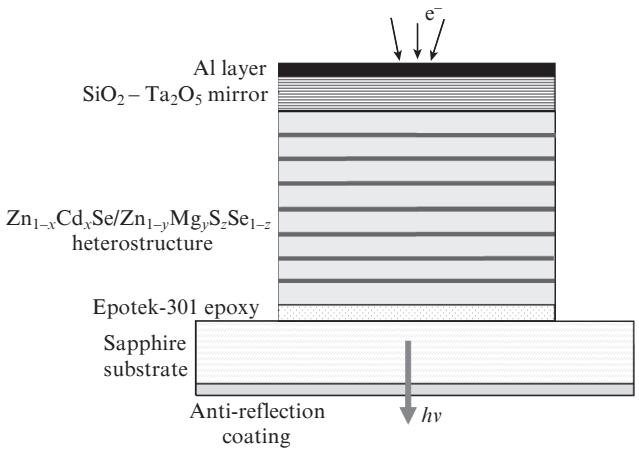

Figure 2. Gain chip of the laser.

Whether or not lasing was achieved depended significantly on the quality of the structures. As in the case of microcavity lasers, it was important to meet requirements for the structure period and to achieve an effective carrier transport from the barriers to the QWs and high emission efficiency at room temperature [7, 9]. At the same time, the quality of the growth surface of the heterostructure for external feedback mirror lasers must meet more stringent requirements than that of the heterostructure for microcavity lasers. Whereas laser action in microcavities can be achieved at rms surface roughness values, σ, within 10 nm, the σ of an external mirror cavity should not exceed 2 nm (see below). In the case of II–VI based epitaxial heterostructures, this is a serious technical problem. Figure 3 is an atomic force microscopy (AFM) image of the surface of the structure in question (Solver P-47 instrument, intermittent contact mode). The rms roughness value σ was determined to be 1.47 nm. Note that we failed to achieve lasing in structures with $\sigma > 3$ nm.

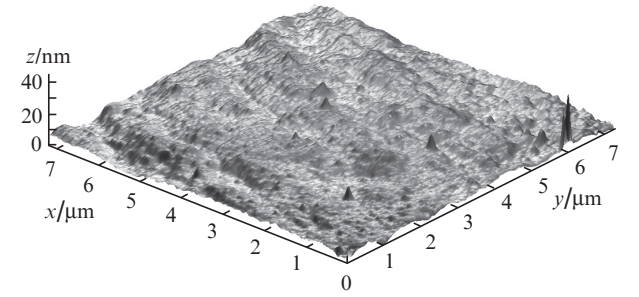

Figure 3. AFM image of the surface of the structure studied (intermittent contact mode).

It is also worth noting that the growth units we used failed to ensure high uniformity of the layers in thickness. Because of this, the results below were obtained on relatively small areas, where the resonance condition for the structure period was met.

Emission spectra were measured on an MDR-4 spectrometer equipped with a linear CCD array detector (Institute of Spectroscopy, Russian Academy of Sciences, Troitsk). The far-field intensity distribution of the laser beam was photographed with a Canon EOS 350 digital camera having no lens, placed 40 cm from the laser. Light pulses were detected by a calibrated FEK-29 coaxial photodiode. Its signal was fed to a TDS-2024 oscilloscope. The electron beam current I_e was measured using a tantalum plate current collector. The electron beam used for pumping had a narrow electron energy (E_e) distribution. E_e was varied by changing the anode–cathode voltage. In evaluating the pump power absorbed by the gain chip of the laser, P_e, we took into account factors related to secondary electron emission from the tantalum plate and to the fraction of energy carried by reflected and secondary electrons away from the gain chip. The true electron beam current exceeded the current measured using the tantalum plate by about a factor of 2. Note that about 25% of the incident electron beam energy was carried away by reflected and secondary electrons. In view of this, the absorbed pump power was estimated as $P_e = 1.5 I_e E_e$. The electron beam scan rate along a horizontal segment was varied in the range $(4–8)\times10^4$ cm s^{-1}. The electron beam spot diameter, d_e, was controlled by varying the current through the focusing electromagnetic lens. The minimum spot diameter (fine focusing) was ~25 μm at an electron energy $E_e = 40$ keV and increased with decreasing E_e and increasing I_e.

3. Experimental results and discussion

Figure 4 shows the emission spectrum of the heterostructure laser, which emits in the blue spectral region. We used an external mirror of radius $r = 30$ mm and reflectivity $R = 0.97$. Lasing was observed at cavity lengths L_c from 30 to 25 mm. Below the lasing threshold, the emission bandwidth exceeded 20 nm. The modulation seen in the spectrum is due to the

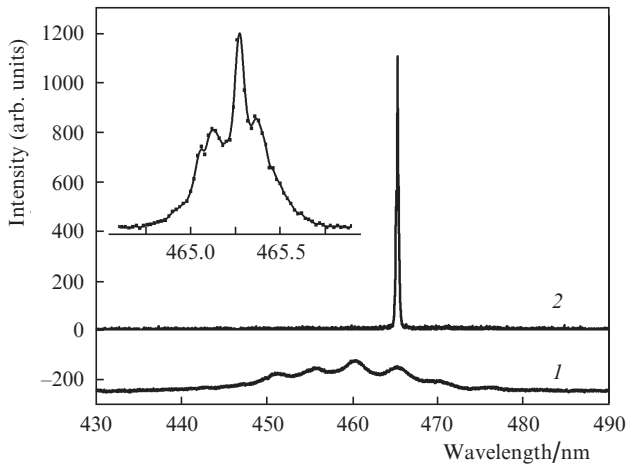

Figure 4. Emission spectrum of the laser at $E_e = 40$ keV (*1*) below and (*2*) above the lasing threshold. Inset: laser emission line recorded at a higher resolution.

internal modes of the microcavity formed by the heterostructure faces. Above threshold, lasing was observed predominantly on one line, at 465 nm, with a full width at half maximum (FWHM) under 0.3 nm. At a small detuning of the structure period from the resonant periodic gain condition, we were able to obtain lasing on two longitudinal modes of the microcavity. A spectrum taken using five pulses comprised several lines about 0.1 nm in width. The structure of the lasing spectrum seems to originate from the pulse-to-pulse instability of the laser emission line.

Figure 5 shows the far-field intensity distributions of the laser beam at cavity lengths of 28.5 and 29.9 mm. When the cavity length approached 30 mm (which corresponded to an unstable semiconcentric cavity), the beam divergence increased markedly. Lasing disappeared when the field distribution width on the external mirror was comparable to the size of the mirror. In the far-field patterns, one can see interference fringes due to the laser beam reflection from the outer surface of the external mirror substrate. That surface had no anti-reflection coating.

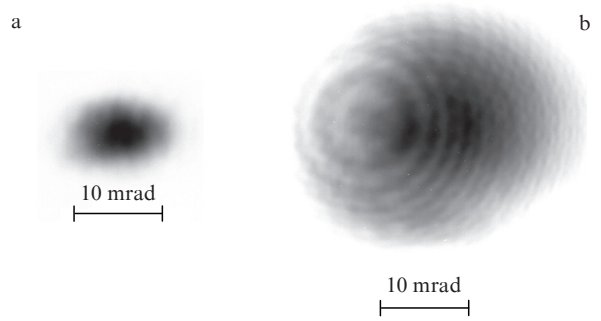

Figure 5. Far-field intensity distributions of the laser beam at cavity lengths of (a) 28.5 and (b) 29.9 mm and an external mirror radius of 30 mm.

The total divergence angle of the stable cavity (L_c = 28.5 mm) in the vertical direction, normal to the electron beam scan direction, was 7 mrad. Even though the directivity pattern was not quite symmetric, we believe that the laser emitted on the fundamental transverse mode. The 1/e fundamental mode diameter on the surface of the structure, d_m, and on the external mirror, d_{mir}, can be estimated as [10]

$$d_m = \left[\frac{4\lambda^2 L_c^2}{\pi^2}\frac{(r-L_c)}{L_c}\right]^{1/4}, \quad d_{mir} = \left[\frac{4\lambda^2 L_c^2}{\pi^2}\frac{L_c}{(r-L_c)}\right]^{1/4}. \qquad (1)$$

At L_c = 28.5 mm, we obtain from (1) $d_m \approx 40$ μm and $d_{mir} \approx$ 190 μm. The focal length of the scattering lens formed by the external mirror substrate is 65 mm. This lens increases the divergence angle of the laser beam by 0.19/65 ≈ 3 mrad. Given this, we take the true divergence of the laser beam to be 4 mrad, which corresponds to the divergence of a Gaussian beam [11]: $\lambda/(\pi d_m) = 4$ mrad.

Figure 6 shows a laser pulse trace obtained at a cavity length of 28.5 mm and external mirror radius of 30 mm. At a scan rate $v_{sc} = 8\times10^4$ cm s^{-1}, the pulse FWHM was 25 ns and the width of base was 40 ns. Under the assumption that the loss in the cavity was mainly the useful loss through the output coupler, an upper estimate of the photon lifetime in the lasing mode is 5 ns. The lifetime is even shorter if there are other losses. Therefore, it seems likely that lasing has time

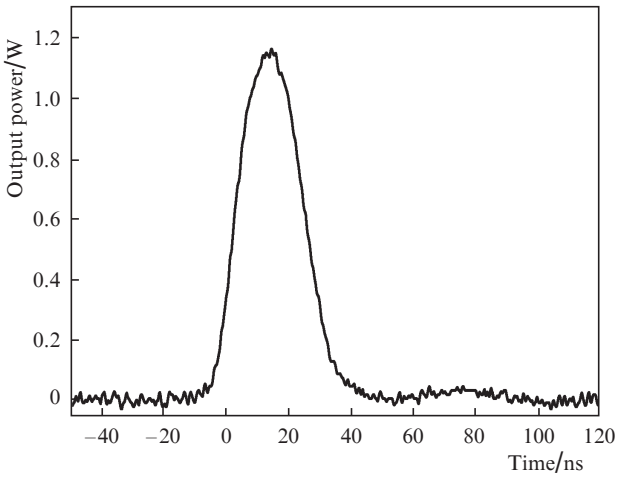

Figure 6. Laser pulse trace at a cavity length of 28.5 mm and an external mirror radius of 30 mm.

enough to reach a steady state. Note that, in the case of fine focusing, the mode excitation time can be estimated at $t_p \approx (2d_e + d_m)/v_{sc}$ = 110 ns, which is markedly longer than the observed pulse duration. This suggests that a lasing threshold emerges only when the excitation region almost completely corresponds to transverse propagation of the fundamental cavity mode.

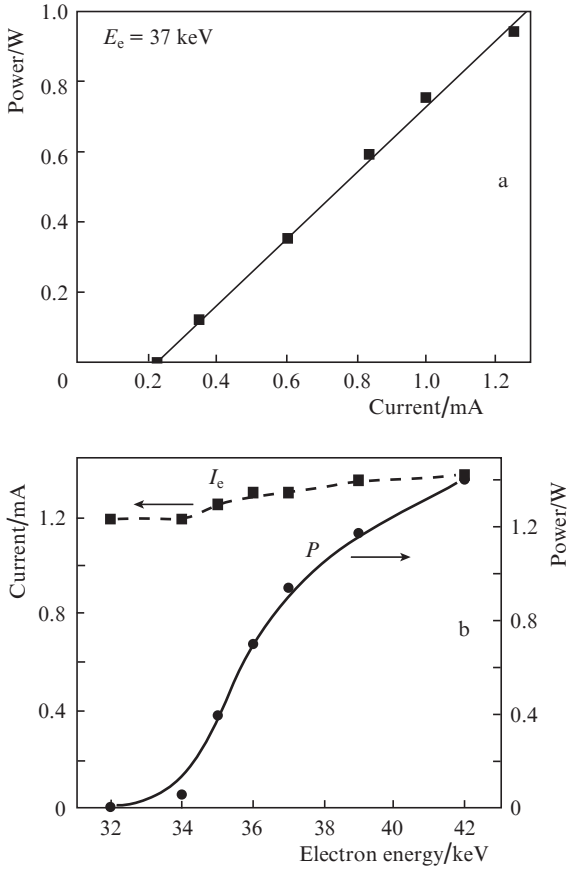

Figure 7. (a) Peak laser output power P as a function of electron beam current I_e at E_e = 37 keV; (b) output power and electron beam current as functions of electron energy E_e.

The laser output power as a function of electron beam current and electron energy is shown in Fig. 7. At each combination of the beam current and electron energy, we varied the electron beam diameter d_e and measured the maximum output power. The maximum in power corresponded to a d_e value roughly equal to the transverse size of the fundamental cavity mode, d_m. Above the lasing threshold, the output power was an almost linear function of electron beam current, reaching 0.95 W at E_e = 37 keV and I_e = 1.2 mA (the highest possible current in the experimental setup used).

The threshold current for lasing was ~0.2 mA at E_e = 37 keV. At $d_m \approx 40$ μm, this corresponds to a current density of 16 A cm^{-2} (or to a peak absorbed pump power density of 885 kW cm^{-2}), which is about seven times that in an analogous GaInAs/GaAs heterostructure laser with 13 QWs [12]. Taking into account the difference in the number of QWs, we find that the lasing threshold per QW in the Zn(Cd)Se/ZnMgSSe structure is about three times higher. This increased threshold is not surprising given that the lasing threshold differs little from the population inversion threshold, which increases with electron and hole effective masses. However, the threshold pump power density in this study considerably exceeds the 2 kW cm^{-2} demonstrated experimentally for optically pumped GaInAs/GaAs semiconductor lasers [10]. We expect that, by optimising the number of QWs, improving the quality of the heterostructure, and using a higher finesse cavity, we will be able to lower the lasing threshold by several times. Nevertheless, even after optimisation the lasing threshold will considerably exceed the level at which cw lasing is possible.

As seen in Fig. 7b, the output power of the laser strongly depends on electron energy. At low electron energies (E_e < 32 keV), no lasing took place because of the significant electron energy loss in the high-reflectivity mirror the laser was pumped through and because of the large mismatch between the excitation depth and the thickness of the gain structure. Indeed, the nominal thickness of the mirror was 1.3 μm, the thickness of the gain structure was 5.45 μm, and the effective electron beam excitation depth z_0 was about 2.5 μm at E_e = 32 keV [13]. The effective excitation depth is here taken to mean the depth of uniform excitation at the electron beam current density corresponding to the maximum in the ionisation curve and the total excitation energy corresponding to the area (integral) under the ionisation curve.

The highest peak laser output power, 1.4 W, was obtained at E_e = 42 keV ($z_0 \approx 4$ μm), but even at such electron energies the excitation region was not sufficiently matched to the active region of the structure. Unfortunately, at higher electron energies (a better match between the excitation region and the thickness of the active region of the heterostructure) we observed rapid degradation of the laser because the electron beam penetrated into the epoxy layer and broke it down. The point is that the total length of the rectified electron trajectory, R_e, exceeds z_0 by about a factor of 2.5 and is 10 μm at E_e = 42 keV. There are several ways to solve this problem. One way is to insert a passive layer of appropriate thickness (about 5 μm) between the gain chip and epoxy layer [14]. Another way is to bond a structure with a high-reflectivity coating to a metallic substrate by metallic solder [7, 12]. The laser emission is then outcoupled from the structure through the surface under irradiation, and the structure is excited through its free surface, which allows the electron energy to be reduced to 14 keV [12].

The output power obtained in this study, 1.4 W, is lower than that achieved at E_e = 42 keV with a microcavity laser based on the same heterostructure (4 W) [7]. However, Tiberi et al. [7] used a rather transparent output coupler, with R = 0.915, instead of the 0.97 in this study. If there are internal losses in the structure, such a difference between the reflectivities of the output couplers may have a significant effect on the output power. Moreover, the disk laser has extra losses related to the roughness of the growth surface of the structure. Indeed, the reflectivity of a rough surface for a plane wave can be written in the form [15, 16]

$$R_r = R_0 \exp\left[-\left(\frac{4\sigma N}{\lambda}\right)^2\right], \quad (2)$$

where R_0 is the reflectivity of a flat surface and N is the refractive index of the medium the plane wave comes from. In our case, R_0 = 1, N = 1.53, λ = 465 nm and σ = 1.47 nm (the wave is incident on the surface from the epoxy layer). Therefore, R_r = 0.995, i.e. the scattering loss is not very high. At the same time, a significantly different situation may occur at high roughness values, as mentioned above. Figure 8 presents R vs. σ data. For σ > 4 nm, the scattering loss will exceed the useful loss.

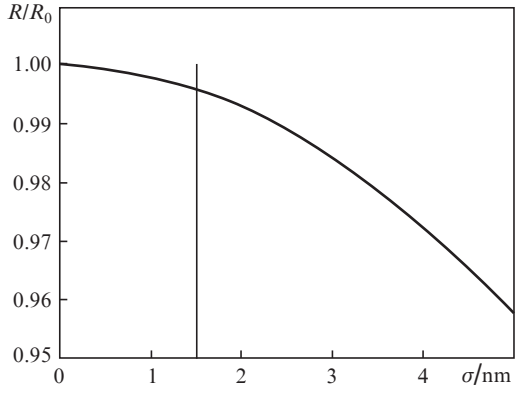

Figure 8. Normalised reflectivity as a function of rms surface roughness σ for plane waves. The vertical line indicates the σ of the structure studied (σ = 1.47).

Relation (2) is only valid for plane waves. This constraint is not strictly fulfilled for lasers with limited transverse dimensions of the lasing mode, especially for microcavity lasers. The divergence of such lasers exceeds 15° and is essentially independent of the transverse size of the excitation region. Their active region breaks down into several independent regions, which is the consequence of the particular kinetics of the approach to steady-state lasing and is unrelated to any transverse inhomogeneity in the gain medium or mirrors. In particular, in an external feedback mirror disk laser the same active region emits coherently at transverse dimensions over 100 μm.

Turning back to the surface roughness of the gain structure, it is worth pointing out that, in lasers with a large beam divergence, a second important roughness parameter, in addition to σ, is the characteristic transverse roughness size. This parameter influences the angle within which light reflected from a rough surface is mainly scattered. Fourier analysis of

the surface represented in Fig. 3 indicates that the transverse size of surface asperities, ξ, is ~1 μm. This means that the surface will scatter approximately in an angle $\lambda/\xi = 15°$. In a microcavity, such scattering will cause no significant extra losses. In an external feedback mirror disk laser, the beam divergence may reach 4–5 mrad, and scattering from a rough surface (with $\sigma > 4$ nm at $R = 0.97$) will then cause significant losses.

4. Conclusions

We have demonstrated for the first time blue-green emission from a Zn(Cd)Se/ZnMgSSe QW semiconductor disk laser without frequency doubling. At an electron energy of 42 keV, the peak output power reached 1.4 W. The laser wavelength was 465 nm, and the pulse duration was about 25 ns FWHM. In a stable cavity, the beam divergence angle was within 10 mrad. An essential condition for lasing was high quality of the growth surface of the heterostructure, which had an rms roughness value of 1.47 nm. At the same time, the threshold pump power density obtained (~900 kW cm^{-2}) is too high for room-temperature cw operation. Nevertheless, electron beam pumping can be a viable alternative in systems where beam scanning is needed. Compared to microcavity lasers proposed earlier, disk lasers pumped by a scanned electron beam will offer higher beam quality.

Acknowledgements. We are grateful to B.M. Lavrushin and Yan K. Skasyrsky for helpful discussions and for their assistance with this study.

This work was supported by the RF Ministry of Education and Science (federal targeted programme The Scientists and Science Educators of Innovative Russia, State Contract No. 14.740.11.1368), the Physical Sciences Division of the Russian Academy of Sciences (basic research programme Fundamental Aspects of the Physics and Technology of Semiconductor Lasers As Cornerstones of Photonics and Quantum Electronics) and the Russian Foundation for Basic Research (Grant Nos 10-02-00741, 11-07-001195 and 11-02-12190-ofi-m).

References

1. Kuznetsov M., Hakimi F., Sprague R., Mooradian A. *IEEE Photonics Technol. Lett*., **9**, 1063 (1997).
2. Tropper A.C., Hoogland S. *Prog. Quantum Electron*., **30**, 1 (2006).
3. Okhotnikov O.G. *Kvantovaya Elektron*., **38**, 1083 (2008) [*Quantum Electron*., **38**, 1083 (2008)].
4. Chilla J., Butterworth S., Zeitchel A., Charles J., Caprara A., Reed M., Spinelli L. *Proc. SPIE Int. Soc. Opt. Eng*., **5332**, 143 (2004).
5. Hastie J.E., Morton L.G., Kemp A.J., Dawson M.D., Krysa A.B., Roberts J.S. *Appl. Phys. Lett*., **89**, 061114 (2006).
6. Kozlovskii V.I., Lavrushin B.M., Skasyrsky Ya.K., Tiberi M.D. *Kvantovaya Elektron*., **39**, 731 (2009) [*Quantum Electron*., **39**, 731 (2009)].
7. Tiberi M.D., Kozlovsky V.I., Kuznetsov P.I. *Phys. Status Solidi B*, **247**, 1547 (2010).
8. Kozlovsky V.I., Martovitsky V.P. *Phys. B*, **404**, 5009 (2009).
9. Bondarev V.Yu., Kozlovskii V.I., Krysa A.B., Popov Yu.M., Skasyrsky Ya.K. *Kvantovaya Elektron*., **34**, 919 (2004) [*Quantum Electron.*, **34**, 919 (2004)].
10. Kuznetsov M., Hakimi F., Sprague R., Mooradian A. *IEEE J. Sel. Top. Quantum Electron*., **5**, 561 (1999)
11. Karlov N.V. *Lectures on Quantum Electronics* (Boca Raton: CRC, 1992; Moscow: Nauka, 1983).
12. Kozlovsky V.I., Lavrushin B.M., Okhotnikov O.G., Popov Yu.M. *Trudy III Simp. po kogerentnomu izlucheniyu poluprovodnikovykh soedinenii i struktur* (Proc. III Symp. on Coherent Emission from Compound Semiconductors and Semiconductor Structures) (Moscow: FIAN, 2011) pp 210–216.
13. Bogdankevich O.V., Darznek S.A., Eliseev P.G. *Poluprovodnikovye lazery* (Semiconductor Lasers) (Moscow: Nauka, 1976) p. 199.
14. Bondarev V.Yu., Kozlovsky V.I., Krysa A.B., Roberts J.S., Skasyrsky Ya.K. *J. Cryst. Growth*, **272**, 559 (2004).
15. Shin H.-E., Ju Y.-G., Song H.-W., Song D.-S., Han I.-Y., Ser J.-H., Ryu H.-Y., Lee Y.-H. *Appl. Phys. Lett.*, **72**, 2205 (1998).
16. Kozlovskii V.I., Trubenko P.A., Korostelin Yu.V., Roddatis V.V. *Fiz. Tekh. Poluprovodn*., **34**, 1237 (2000).